THE JOURNAL OF BIOLOGICAL CHEMISTRY
Vol. 279, No. 37, Issue of September 10, pp. 38936–38942, 2004
Printed in U.S.A.

Identification of Distinct N-terminal Truncated Forms of Prion Protein in Different Creutzfeldt-Jakob Disease Subtypes*

Received for publication, May 17, 2004, and in revised form, July 7, 2004
Published, JBC Papers in Press, July 9, 2004, DOI 10.1074/jbc.M405468200

Gianluigi Zanusso‡, Alessia Farinazzo‡, Frances Prelli§, Michele Fiorini‡, Matteo Gelati‡, Sergio Ferrari‡, Pier Giorgio Righetti¶, Nicolò Rizzuto‡, Blas Frangione§, and Salvatore Monaco‡‖

From the ‡Departments of Neurological and Visual Sciences, Section of Neurology and ¶Agricultural and Industrial Biotechnologies, University of Verona, 37134 Verona, Italy and the §Department of Pathology, New York University Medical Center, New York, New York

In prion diseases, the cellular prion protein (PrP^C) is converted to an insoluble and protease-resistant abnormal isoform termed PrP^{Sc}. In different prion strains, PrP^{Sc} shows distinct sites of endogenous or exogenous proteolysis generating a core fragment named PrP27–30. Sporadic Creutzfeldt-Jakob disease (sCJD), the most frequent human prion disease, clinically presents with a variety of neurological signs. As yet, the clinical variability observed in sCJD has not been fully explained by molecular studies relating two major types of PrP27–30 with unglycosylated peptides of 21 (type 1) and 19 kDa (type 2) and the amino acid methionine or valine at position 129. Recently, smaller C-terminal fragments migrating at 12 and 13 kDa have been detected in different sCJD phenotypes, but their significance remains unclear. By using two-dimensional immunoblot with anti-PrP antibodies, we identified two novel groups of protease-resistant PrP fragments in sCJD brain tissues. All sCJD cases with type 1 PrP27–30, in addition to MM subjects with type 2 PrP27–30, were characterized by the presence of unglycosylated PrP fragments of 16–17 kDa. Conversely, brain homogenates from patients VV and MV with type 2 PrP27–30 contained fully glycosylated PrP fragments, which after deglycosylation migrated at 17.5–18 kDa. Interestingly, PrP species of 17.5–18 kDa matched deglycosylated forms of the C1 PrP^C fragment and were associated with tissue PrP deposition as plaque-like aggregates or amyloid plaques. These data show the presence of multiple PrP^{Sc} conformations in sCJD and, in addition, shed new light on the correlation between sCJD phenotypes and disease-associated PrP molecules.

Transmissible spongiform encephalopathies, or prion diseases, are mammalian neurodegenerative diseases leading to rapidly progressive neurological dysfunction (1). They include sheep scrapie, bovine spongiform encephalopathies, and Creutzfeldt-Jakob disease in humans (1–3). In these disorders, the host cellular prion protein (PrP^C)[1] is converted to an abnormal conformer (PrP^{Sc}) biochemically characterized by detergent insolubility and relative resistance to protease treatment (4). Whereas PrP^C is sensitive to proteinase K (PK) digestion, PrP^{Sc} is cleaved within the N-terminal region and generates N-terminally truncated species referred to as PrP 27–30 (5). PrP^C and PrP^{Sc} undergo intracellular proteolytic cleavages with generation of distinct C-terminal fragments. PrP^C is cleaved at amino acids 110/111 and 90, producing an 18-kDa fragment named C1 and a larger fragment of ~20 kDa (6, 7). Conversely, PrP^{Sc} is cleaved within the N-flexible region with formation of a fragment referred to as C2, sharing its conformation with PrP27–30 (6, 7). Recently, C-terminal PrP fragments of ~11–12 kDa and 12–13 kDa have been identified in iatrogenic (8) and sporadic Creutzfeldt-Jakob disease (sCJD) (8, 9).

Neuropathological hallmarks of transmissible spongiform encephalopathies include spongiosis, neuronal loss, and gliosis accompanied by PrP^{Sc} deposition at synaptic locations and at the rims of vacuoles or as large extracellular amyloid plaques and plaque-like aggregates (10). Different patterns of PrP deposition and intracerebral regional distribution of lesions are explained by the existence of prion strains with identifiable biological properties and distinctive physicochemical features of PrP^{Sc} (1).

sCJD has an annual incidence of ~1–1.5 per million worldwide and a still unknown etiology; prevailing hypotheses suggest that the disorder is triggered by pathogenic somatic mutations in the prion protein gene (*PRNP*) or by random spontaneous changes in PrP^C conformation (11). However, there is concern that some sCJD cases could be secondary to environmental exposure, case-to-case transmission, or unnoticed food chain contamination, as suggested by the occurrence of atypical phenotypes, spatiotemporal disease clusters (12), and the increased incidence of the disorder recently observed in Switzerland (13). Because of the variability in clinical presentation, signs at evolution, and neuropathological changes, the disorder with the double eponym Creutzfeldt-Jakob should be properly called syndrome rather than disease. Different sCJD phenotypes largely correlate with the *PRNP* codon 129 genotype, a site of methionine or valine polymorphism, and distinct PrP^{Sc} types (14) currently classified according to the molecular

* This work was supported by grants from the Italian Ministry of Health in collaboration and with the contribution of the Istituto Superiore di Sanità ("Search for infection-related endogenous or exogenous factors in the cerebrospinal fluid of patients with transmissible spongiform encephalopathy" and "Study of pathogenic mechanisms in neurodegenerative disorders for the diagnosis and development of therapeutic approaches.") and from National Institutes of Health Grant AR02584 (to B. F.). The costs of publication of this article were defrayed in part by the payment of page charges. This article must therefore be hereby marked "*advertisement*" in accordance with 18 U.S.C. Section 1734 solely to indicate this fact.

‖ To whom correspondence should be addressed: Dept. of Neurological and Visual Sciences, Section of Neurology, Policlinico G. B. Rossi, P.le L. A. Scuro, 10, 37134 Verona, Italy. Tel.: 39-045-8074286; Fax: 39-045-585933; E-mail: salvatore.monaco@mail.univr.it.

[1] The abbreviations used are: PrP^C, cellular prion protein; PrP^{Sc}, scrapie isoform of prion protein; sCJD, sporadic Creutzfeldt-Jakob disease; MM, diglycosylated PrP^{Sc} species; MV, monoglycosylated PrP^{Sc} species; VV, unglycosylated PrPSc species; PK, proteinase K.

mass of their PrP27–30 core fragment in turn reflect the tertiary structure of PrP^{Sc}. However, controversial results have been obtained by different authors who have proposed the classification of sCJD PrP27–30 into two (14) and four types (15). Two main limitations of these studies are (i) the use of a relatively crude technique of protein separation, such as SDS-PAGE, and (ii) the detection of PrP species with an antibody recognizing the N-terminal 109–112 epitope, which precludes the recognition of PrP molecules lacking this region.

Here we studied 32 subjects, with definite sCJD of all genotypes at *PRNP* codon 129 and with different PrP^{Sc} types, to characterize C-terminal PrP^{Sc} fragments in distinct disease phenotypes and host genotypes. Brain homogenates resolved by SDS-PAGE and two-dimensional electrophoresis were immunoblotted with anti-PrP antibodies recognizing epitopes located in the N-terminal and C-terminal regions. Here we report the detection of novel truncated PrP^{Sc} species in association with distinct PrP27–30 types. In addition, we provide evidence that sCJD phenotypes with PrP amyloid plaques or plaque-like deposits are associated with pathological PrP species matching the so-called C1 PrP^{C} fragment.

MATERIALS AND METHODS

Patients and Tissue Samples—Thirty-two cases of definite sCJD, diagnosed according to current criteria, were investigated in the present study. Clinical, epidemiological, molecular, and pathological data are reported in Table I; postmortem intervals ranged from 4 to 30 h. Fresh brain tissues obtained at autopsy were stored frozen at −80 °C until use. Genomic DNA, extracted from frozen brain tissues, was searched for *PRNP* mutations and polymorphic Met/Val at codon 129. Neuropathological and immunohistochemical studies were performed as described previously (16).

Immunoblot Analysis—Tissue samples from different brain regions, including the frontal and occipital cortices, thalamus, basal ganglia, and cerebellum, were dissolved in 9 volumes of lysis buffer (100 mM NaCl, 10 mM EDTA, 0,5% Nonidet P-40, 0.5% sodium deoxycholate, 10 mM Tris) at pH 5, 7.4, and 8 and clarified by centrifugation at 1,000 × *g* for 10 min. The supernatant was stored at −80 °C, whereas the pellet was discarded. Detergent-insoluble fractions were obtained by 2 cycles of centrifugation at 100,000 × *g* for 90 min, as reported previously (17). Protease resistance was assayed by incubating sample aliquots containing 40 μg of total protein with 100 μg/ml of PK (Roche Applied Science) for 1 h at 37 °C. The digestion was blocked by the addition of phenylmethylsulfonyl fluoride to 3 mM. The samples were deglycosylated with *N*-glycosidase F (PNGase F) according to the manufacturer's instructions (Roche Applied Science). Proteins were dissolved in sample buffer (3% SDS, 3% β-mercaptoethanol, 2 mM EDTA, 10% glycerol, 62.5 mM Tris, pH 6.8) and boiled for 5 min. An equivalent of 0.4 mg of wet tissue was loaded onto 12% SDS-PAGE gels and then transferred onto polyvinylidene difluoride membrane (Immobilon P, Millipore) for 2 h at 60 V. The membranes were blocked with 1% nonfat dry milk in TBST (10 mM Tris, 150 mM NaCl, 0.1% Tween 20, pH 7.5) for 1 h at 37 °C and incubated overnight at 4 °C with appropriate antibodies. Blots were developed with an enhanced chemiluminescence system (ECL, Amersham Biosciences), and PrP was visualized on autoradiography film (Hyperfilm, Amersham Biosciences). The following anti-PrP monoclonal antibodies were used: 3F4, recognizing human PrP residues 109–112 (1:30000); 6H4, binding an epitope between amino acids 144–152 (Prionics, 1:5000), and SP-214, directed against the 214–231 sequence of human PrP (1:1000) (7).

Two-dimensional Gel Electrophoresis—For isoelectric focusing, using immobilized pH gradients in the first dimension, 8-cm long precast gels with a linear pH range of 3–10 were used. Before isoelectric focusing, the dry gels were swollen for 16 h in 125 μl of buffer (8 M urea, 5% β-mercaptoethanol, 2% Nonidet P-40, and 2% ampholyte) containing 10 μl of sample (an equivalent of 1 mg of wet tissue). Isoelectric focusing was carried out at 20 °C for 30 min with 500 V, 30 min with 1000 V, and 1 h with 4000 V in a cooled horizontal electrophoresis unit (IPGphor, Amersham Biosciences). For the second dimension, the immobilized pH gradient strips were equilibrated for 15 min in 50 mmol/liter Tris-HCl, 6 mol/liter urea, 10% glycerol, 2% SDS, and a trace of bromphenol blue and loaded in a 12% SDS-PAGE as described previously (17). Immunoblotting was performed as described above.

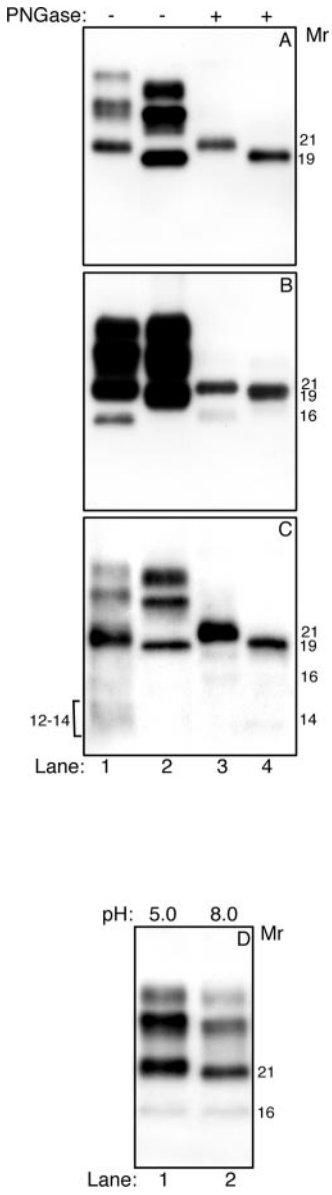

FIG. 1. **Western immunoblot of PrP27–30 and truncated PrP fragments in sCJD brains.** Immunoblot analysis of PrP27–30 in frontal cortex homogenates of sCJD subjects with type 1 (*A–C*, *odd lanes*) or type 2 PrP^{Sc} (*A–C*, *even lanes*), either untreated (−) or treated (+) with PNGase. PK-resistant PrP forms were detected on immunoblots with anti-PrP antibodies 3F4 (*A*), 6H4 (*B*), and SP-214 (*C*). The 6H4 antibody recognizes a 16–17-kDa unglycosylated C-terminal PrP fragment in association with type 1 PrP27–30 (*B, lane 1*) and an 18-kDa form in PNGase-treated samples from sCJD with type 2 PrP27–30 (*B, lane 3*). Lower truncated molecular mass PrP forms are detected on the immunoblot with SP-214, mostly in association with type 1 PrP27–30 (*C*). Immunoblot with 6H4 of frontal cortex homogenate from an MM subject with pH-sensitive PrP^{Sc} shows different patterns of type 1 PrP27–30 migration after serial PK digestion in lysis buffer at pH 5 (*D, lane 1*) and pH 8 (*D, lane 2*), respectively. Molecular mass is shown in kDa.

RESULTS

Immunoblot Typing of PrP27–30—Brain homogenates from subjects either homozygous or heterozygous at *PRNP* codon 129 showed two distinct patterns of PrP^{Sc} electrophoretic migration following treatment with proteinase K and immunoblot with 3F4. In 18 sCJD cases (15 MM, 1 MV, 2 VV) three major bands corresponding to di-, mono-, and unglycosylated PrP^{Sc} species migrated at 30, 25, and 21 kDa (Fig. 1*A*, *lane 1*), whereas in 14 cases (3 MM, 5 MV, and 6 VV) the bands were detected at 28-, 23-, and 19-kDa zones (Fig. 1*A*, *lane 2*). In each

TABLE I
Demographic, molecular, and phenotypic features in SCJD cases

Cases	Mean age	Sex	Codon 129 PrP^{Sc} fragment	Symptoms at onset	Duration	Susceptibility to pH changes	Pattern of PrP immunostaining
No.	*years*				*months*		
9	66.3 (±7)	6M, 3F	Met/Met 21 kDa	Hallucinations, dementia, ataxia	6.2 (±4.8)	Yes	Synaptic deposits
6	61.8 (±9.5)	3M, 3F	Met/Met 21 kDa	Hallucinations, ataxia, dementia	9.1 (±8.7)	Low	Synaptic deposits
1	69	M	Met/Val 21 kDa	Apraxia, aphasia	20	Low	Synaptic deposits; multiple clusters in the cerebellum
2	48.5 (±16.3)	2 M	Val/Val 21 kDa	Psychiatrics disturbances, dementia, ataxia	13.5	Yes/Low	Synaptic deposits
3	60.6 (±1.1)	1M, 2F	Met/Met 19 kDa	Dementia	16 (±3.4)	No	Perivacuolar coarse deposition
5	63.4 (±9.1)	3M, 2F	Met/Val 19 kDa	Ataxia, extrapiramidal signs, dementia	14.8 (±18.6)	No	Perineuronal and axonal deposition. Plaque-like and Kuru plaques
6	70 (±7.1)	2M, 4F	Val/Val 19 kDa	Ataxia	7 (±2.6)	No	Perineuronal and axonal deposition Plaque-like deposition

group, following deglycosylation, the three forms (hereafter referred to as the "PrP^{Sc} triplet") were reduced to the size of the unglycosylated fragment corresponding to 21 and 19 kDa (Fig. 1*A*, *lanes 3* and *4*). These PrP^{Sc} species correspond to type 1 and type 2 PrP^{Sc}, according to the nomenclature used by others (14).

Immunoblot of C-terminal PrP Fragments—In addition to the PrP^{Sc} triplet observed with 3F4, immunoblot with 6H4 showed a PK-resistant PrP^{Sc} band migrating at 16–17 kDa in all subjects with type 1 PrP^{Sc} (Fig. 1*B*, *lanes 1* and *3*); a band with similar electrophoretic mobility was barely detectable also in MM cases with type 2 PrP^{Sc} (MM2) (data not shown). The 16–17-kDa C-terminal fragment was found in untreated brain homogenates and partially recovered in the detergent-insoluble fraction. These biochemical features, combined with the absence of this fragment in normal brains, suggest that this truncated form is mainly generated by an aberrant endogenous PrP^{Sc} cleavage.

In marked contrast, following PK digestion and immunoblot with 6H4, sCJD brains from subjects MV and VV at codon 129 and with type 2 PrP^{Sc} contained only the PrP^{Sc} triplet (Fig. 1*B*, *lane 2*) but not the 16–17-kDa fragment found in cases with type 1 PrP^{Sc} and in MM2 cases. However, after PNGase treatment, PK-digested samples from MV2 and VV2 cases showed an additional band migrating at ~18 kDa (Fig. 1*B*, *lane 4*).

Finally, immunoblot with SP-214 of brain homogenates from different sCJD subtypes showed, in addition to the PrP^{Sc} triplet, several PK-resistant PrP^{Sc} bands, with the lowest molecular mass fragments being detected at ~12 kDa. The pattern of PK-resistant PrP species obtained in cases with type 1 PrP^{Sc} disclosed indistinct banding in a range between 12–17 kDa, either prior to (Fig. 1*C*, *lane 1*) or after deglycosylation (Fig. 1*C*, *lane 3*), whereas in MV2 and VV2 subjects (Fig. 1*C*, *lane 2*), fewer truncated fragments were seen, migrating at 18- and 12-kDa zones after PNGase and PK treatment (Fig. 1*C*, *lane 4*).

Effect of pH on PrP27–30 and on Truncated PrP Fragments—In a previous study, we observed that one type of PrP^{Sc}, detected in the classical form of sCJD, changes its conformation after exposure to acidic and basic pH values (18). This property, likely dependent on the presence of octapeptide repeats in the PrP^{Sc} molecule, enabled us to distinguish two PrP^{Sc} types that share an identical electrophoretic mobility after solubilization in lysis buffer at pH 7.4. Following immunoblot with 3F4, the PK-resistant fragment of 21 kDa, detected in 9 MM subjects and in 1 VV case, migrated slower at pH 5 as compared with the migration observed when samples were solubilized at pH 8 (Table I). In contrast, PrP^{Sc} migration was not consistently modified in 6 MM, 1 MV, and 1 VV cases with type 1 PrP27–30 and in all cases with type 2 PrP27–30. To further clarify the influence of the octapeptide region in determining sensitivity to pH, brain homogenates from each single case of the group sensitive to pH were exposed to consecutive PK digestions, first to acidic and subsequently to basic pH. As expected, the immunoblots with 6H4 showed that, at acidic pH, the main fragment migrated at ~22.5 kDa, and following further digestion at pH 8, it was detected in a 20-kDa zone because of the effect of an additional cleavage. Immunoblots with SP-214, recognizing the 214–231 C-terminal sequence of human PrP, showed similar results (data not shown) thus suggesting that the 22.5 and 20 kDa bands differ at the N terminus and not at the C terminus. Conversely, the electrophoretic migration of the C-terminal fragment of 16–17 kDa was unaffected by serial acidic and basic digestion procedures (Fig. 1*D*, *lanes 1* and *2*), confirming the role of the octapeptide region in conferring PrP^{Sc} susceptibility to conformational changes.

Two-dimensional mapping of PrP isoforms in control and sCJD brains—Recently, we provided a detailed two-dimensional mapping of PrP^{C} glycoforms by using the 3F4 antibody, recognizing a linear epitope expressed in the full-length PrP^{C} and in the C2 fragment (17). When analyzing PrP^{C} in two dimensions, the customary di-, mono-, and unglycosylated bands of the protein, obtained after SDS-PAGE, are separated in several spots according to two independent features: the isoelectric point (which reflects the net charge) and the mobility (determined by the molecular mass). In addition, after two-dimensional separation, each spot can be assigned to glycosylated or unglycosylated species based on its shape, configuration, tail, and smear. Although the 6H4 antibody was unable to detect PrP^{C} molecules after two-dimensional separation of control brain homogenates, the SP-214 monoclonal antibody revealed several glycosylated and unglycosylated PrP forms with faster migrating species being detected at 18 kDa, corresponding to unglycosylated C1 isoforms (Fig. 2*A*). Negative results obtained with 6H4 suggest that this antibody recognizes a conformational rather than a linear PrP epitope and that this epitope is lost after solubilization of PrP in high molar urea. After PNGase treatment, truncated PrP^{C} glycoforms were all reduced into several spots migrating at 20- and 18-kDa zones (Fig. 2*B*), corresponding to PrP fragments referred to as C2 and C1, respectively. Differing from controls, each single

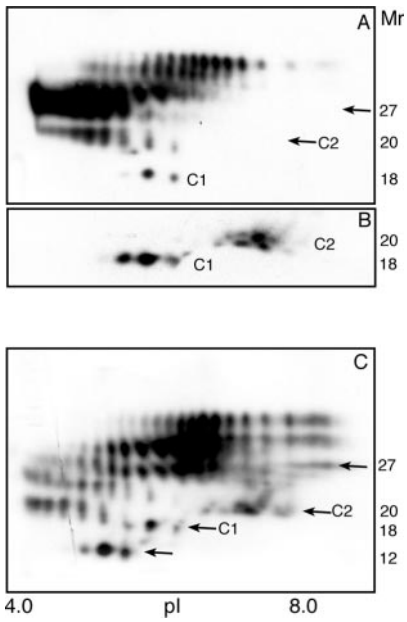

FIG. 2. **Two-dimensional mapping of PrP species in normal and sCJD brains.** Total brain homogenates were resolved by two-dimensional electrophoresis and immunoblotted with SP-214 antibody. In normal human brain glycosylated forms of the full-length PrP^C are resolved into several charge isomers at 35- and 28–30-kDa zones, pI range 5–8. The unglycosylated full-length PrP^C and the C2 fragment (position indicated by *arrows*) were observed in overexposed immunoblots. Acidic glycoforms of 26–27 and 20–22 kDa represent glycosylated species of C2 and C1 fragments (*A*). PNGase treatment reduces truncated PrP^C glycoforms into two zones at 20 and 18 kDa, within pH values of 6.6–7.2 and 4.5–5.3, respectively (*B*). Frontal cortex homogenate from an MV2 sCJD case show the presence of 12–14-kDa molecular mass species of PrP (*arrowhead*) in addition to low molecular mass acidic glycoforms and increased amount of the C2 fragment (*C*, *arrow*). Molecular mass markers are indicated on the *right* and the pI gradient on the *bottom*.

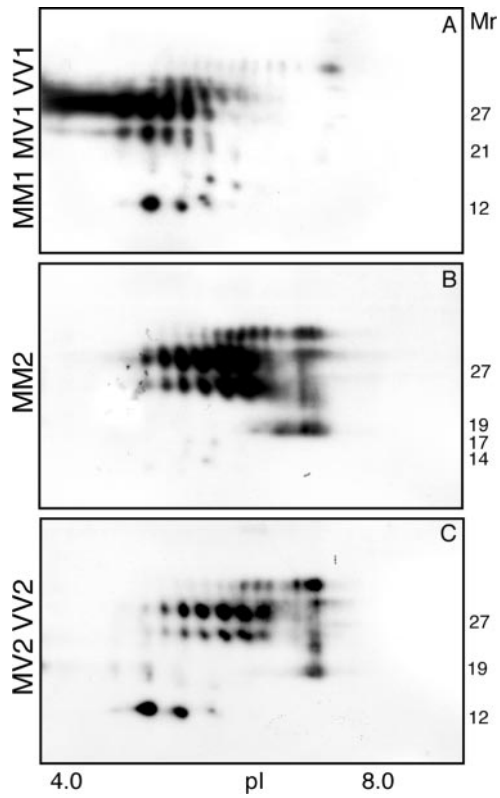

FIG. 3. **Detergent-insoluble PrP-truncated fragments in sCJD brains.** PrP^{Sc} was sedimented by high speed centrifugation as described previously (18) and immunoblotted, after 2-dimensional electrophoresis, with SP-214 monoclonal antibody. Occipital cortex homogenates from MM1 (*A*), MM2 (*B*), and VV2 (*C*) sCJD subjects, representative of molecular groups indicated on the *left*, are shown. In *A*, tissues from a sCJD subject with type 1 PrP27–30 show the presence of 12–14- and 16–17-kDa unglycosylated species, which are also barely detected also in MM2 subjects (*B*). In *C*, only unglycosylated 12–14-kDa spots are seen. Molecular mass markers are shown on the *right*; pI values are indicated on the *bottom*.

homogenate of cortical areas, subcortical nuclei, and cerebellum from sCJD brains showed increased amounts of C2 (migrating at ~21 kDa in cases with type 1 PrP^{Sc} and 19 kDa in those with type 2 PrP^{Sc}) and the presence of additional acidic PrP glycoforms and low molecular mass unglycosylated species. The composition, electrophoretic migration, and relative abundance of these PrP species were different among distinct sCJD subtypes. In particular, sCJD cases of all codon 129 genotypes with type 1 PrP^{Sc} were characterized by the increased expression of unglycosylated PrP forms in a 12–17-kDa zone as opposed to the low abundance of these species in the MM2 subjects and the prominence of low molecular mass acidic PrP glycoforms in MV2 and VV2 subtypes (Fig. 2*C*). Interestingly, truncated PrP species observed in different sCJD subtypes were partially recovered in the detergent-insoluble fraction from different brain areas (Fig. 3, *A–C*).

Two-dimensional Mapping of PK-resistant PrP Fragments in Different sCJD Subtypes—A sextet of molecular sCJD subtypes has been previously recognized based on the combination of two PrP27–30 types and three possible *PRNP* codon 129 genotypes (14). More recent phenotypic classifications propose six variants, which consider MM1 and MV1 cases a single subtype, whereas MM2 subjects are classified in two forms, cortical (MM2C) and thalamic (MM2T), named sporadic fatal insomnia (20). With the exception of sporadic fatal insomnia cases (not available for the present study), all other molecular and phenotypic sCJD subtypes were investigated. PK-treated brain homogenates from subjects with type 1 PrP27–30 of all genotypes showed, in addition to 30-, 25-, and 21-kDa glycoforms containing the 3F4 epitope (Fig. 4, *A*, *C*, and *E*), more acidic SP-214-positive glycoforms of 21–25 kDa and showed several spots migrating at ~16–17- and 12–14-kDa zones, pI 4–5 (Fig. 4, *B*, *D*, and *F*). Some variability was observed among individual cases in the relative intensity and representation of these spots, but their migration and configuration were highly comparable in all cases. Additionally, slight quantitative but not qualitative differences were seen in different brain regions from each case. After deglycosylation and PK-treatment, major glycoforms of 21–30 kDa were reduced to 21 kDa, pI 6.6–7.2, whereas lower molecular mass species were detected at 16–17- and 12–14-kDa zones, pI 4.5–5.5 (Fig. 4, *B′*, *D′*, and *F′*).

In the MM2C group, the 3F4 antibody showed differently glycosylated forms of PrP27–30 (Fig. 4*G*), and barely detectable, faster migrating PrP forms were stained by SP-214 antibody in all sampled brain areas (Fig. 4*H*). After deglycosylation, the 19-kDa PrP^{Sc} core fragment was associated with low amounts of PrP forms showing a migration pattern similar to that found in subjects with type 1 PrP27–30 (Fig. 4*H′*).

Finally, in the MV2 and VV2 groups, major 3F4-positive glycoforms of 29, 25, and 19 kDa (Fig. 4*I*) were associated with small amounts of 12–14-kDa species recognized by the SP-214 antibody (Fig. 4*L*). However, after glycan removal, a set of spots migrating at ~17.5–18 kDa was detected in cortical and subcortical brain regions (Fig. 4*L′*). Based on their pI values and apparent molecular masses, these spots matched the corresponding C1 PrP^C peptides observed after deglycosylation of normal brain homogenates (see Fig. 2*B*).

These results indicate that in MV2 and VV2 cases, glycosyl-

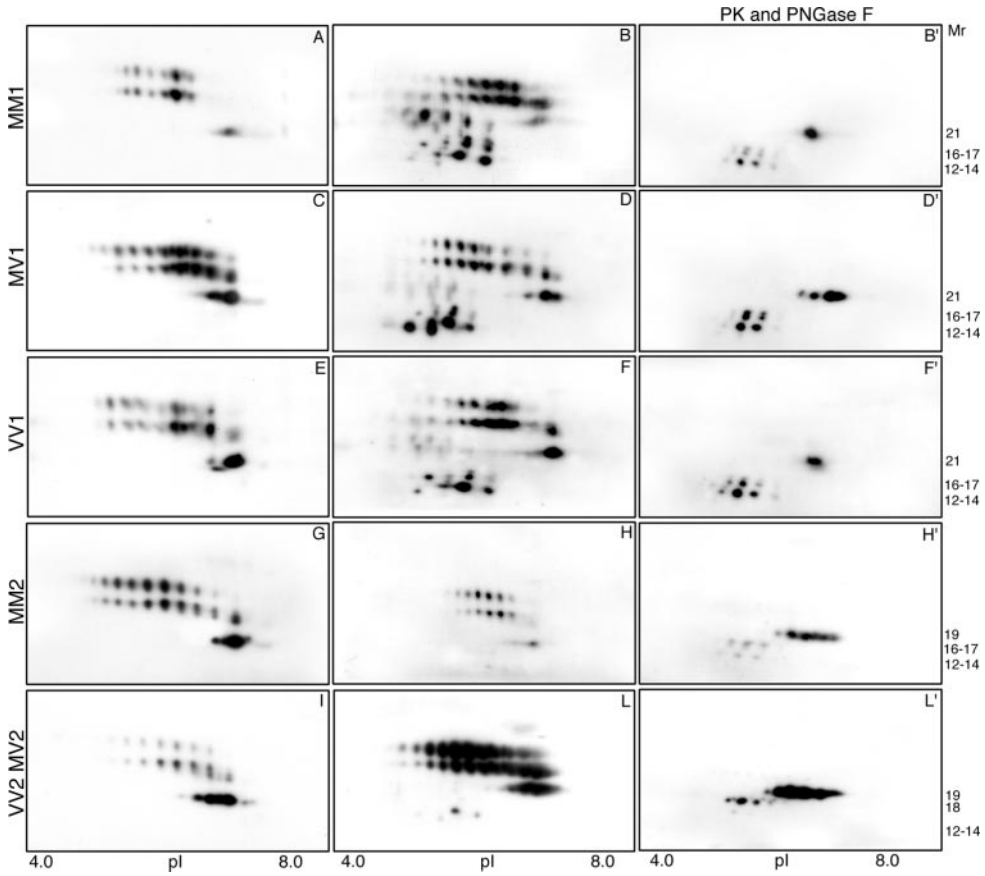

FIG. 4. **Two-dimensional mapping of sCJD brain homogenates after PK treatment and deglycosylation.** PK-resistant PrP products of brain homogenates from representative sCJD subjects were resolved by two-dimensional gel electrophoresis and immunoblotted with the 3F4 antibody (*A*, *C*, *E*, *G*, *I*) and with SP-214 monoclonal antibody before (B, D, F, H, L) and after PNGase treatment (*B′*, *D′*, *F′*, *H′*, *L′*). As shown previously (17), immunoblot with 3F4 of PK-digested frontal cortex homogenates from sCJD subjects show the presence of differently glycosylated PrP charge isomers, with unglycosylated PrP27–30 species migrating at 21 (*A*, *C*, *E*) or 19 kDa (*G*, *I*) in different disease phenotypes. Immunoblot with SP-214 of PK-resistant PrP molecules shows additional unglycosylated PrP spots migrating at 16–17 and 12–14 kDa, in all sCJD subjects with type 1 PrP27–30 (*B*, *D*, *F*); barely detectable spots with an identical migration pattern as those associated with type 1 PrP27–30 are also seen in MM2 subjects (*H*). Conversely, only small amounts of the 12–14-kDa fragments, but not the 16–17-kDa spots, are identified in MV2 and VV2 sCJD cases (*L*). In all sCJD brains with type 1 PrP27–30, PNGase treatment of PK-digested frontal cortex homogenates showed a similar two-dimensional pattern with PrP species being resolved at 21-, 16–17- and 12–14-kDa zones (*B′*, *D′*, *F′*). Again, a similar qualitative pattern of truncated PrP species, with the presence of very small amounts of the 16–17- and 12–14-kDa spots, was seen in MM2 cases (*H′*). On the contrary, two-dimensional maps of PNGase-treated, PK-digested frontal cortex homogenates from MV2 and VV2 subjects disclose several spots at ~18 kDa (*L′*).

ated C1 isoforms acquire PK-resistance, although the possibility that C1-sized fragments are generated upon protease treatment cannot be ruled out. On the contrary, unglycosylated isoforms of C1 detected in both normal and pathological brain homogenates (see Fig. 2, *A* and *C*) lack detergent insolubility (see Fig. 3*C*) and PK-resistance (see Fig. 4*L*) in sCJD brains. The schematic (Fig. 5) depicts different patterns of truncated PrP fragments found in association with distinct molecular sCJD subtypes.

DISCUSSION

The present findings show that: (i) novel truncated PrP fragments are detected in distinct molecular sCJD subtypes; (ii) the combination of PrP27–30 and truncated PrP species identify three biochemical patterns of disease-associated prion protein; (iii) in MV2 and VV2 subtypes of sCJD, glycosylated molecules of the C1 fragment acquire biochemical hallmarks of PrP^{Sc}.

Using sensitive protein separation techniques and Western blot with antibodies recognizing the C-terminal globular domain of prion protein, we have identified new protease-resistant PrP species in brain homogenates from sCJD subjects. These new fragments, detected in the mass interval between 16 and 18 kDa, showed two distinct and highly reproducible electrophoretic patterns, each segregating preferentially with type 1 or type 2 PrP27–30. The electrophoretic migration of these newly identified PK-resistant PrP products is, therefore, intermediate between the unglycosylated PrP27–30 fragment (which is currently used to classify molecular PrP^{Sc} types) and the 12–14 kDa PrP molecules observed in all sCJD subtypes and named CTF 12/13 (9). The immunoblot detection of low molecular mass PrP fragments in untreated whole brain homogenates from sCJD subjects indicates that such fragments are generated by an endogenous proteolytic mechanism. It should also be emphasized that the detergent insolubility of these molecules and the lack of shift in their apparent molecular weight after PK digestion support the view that these PrP species adopt a fully protease-resistant conformation *in vivo*.

Taken together, the present findings point out that multiple abnormal PrP conformers are expressed during the spreading of sCJD strains. This could result from diverse subcellular sites of formation or, alternatively, from the generation of PrP conformers from full-length and N-terminally truncated PrP^{C} precursors. Furthermore, the identification of the 16–17- and 12–14-kDa forms in subjects of all genotypes with type 1 or MM with type 2 PrP^{Sc} suggests that the mechanism involved in the formation of these forms is not influenced by codon 129 and by the type of PrP27–30. Although the three classes of PrP frag-

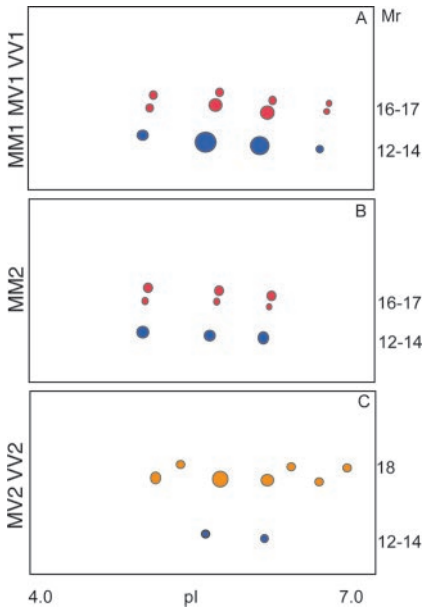

FIG. 5. **Schematic diagram of PK-resistant C-terminal PrP core fragments in sCJD subtypes.** The 16–17-kDa forms, seen in sCJD with type 1 PrP27–30 (*A*) and in MM2 cases (*B*) are represented in *red*, whereas 12–14-kDa species are depicted in *blue*. In MV2 and VV2 groups, C1 PrP^{Sc} spots are shown in *orange* (*C*).

ments characterized in the present study show biochemical properties of pathological PrP, it remains to be determined if they maintain all of the biological properties of PrP^{Sc}.

A further implication of the identification of 16–17-kDa forms is related to the molecular classification of PrP^{Sc} types encountered in sCJD. The influence of several experimental conditions, including pH and EDTA concentration, on the conformation of type 1 PrP^{Sc} and, therefore, on its electrophoretic migration is well known (18, 19). On this basis, we propose the use of conventional Western blot with 6H4 antibody, which is able to detect an accompanying fragment of 16–17 kDa in all cases with type 1 PrP^{Sc}. Such a standardized molecular classification of sCJD would have major implications for epidemiological studies, whereas more sophisticated investigations, such as two-dimensional mapping and PrP sequencing, should be reserved for atypical cases.

To date, the existence of distinct strains of the agent responsible for human prion diseases has been difficult to explain with just the biochemical findings of two main PrP27–30 conformations and with microsequencing analyses showing two truncation patterns in sporadic, inherited, and acquired diseases (21). It is well known that glycans may play a role in the phenotypic determination of some prion conditions, and their role has been recently proposed to explain differences between sporadic fatal insomnia and MM2 sCJD, two conditions sharing PrP27–30 type and *PRNP* codon 129 (22). However, different glycosylation states of PrP^{Sc} cannot fully account for prion diversity. Recent transmission studies of sCJD to transgenic mice show three distinct incubation periods of different sCJD subtypes (23). In particular, inocula from subjects MM1 and MV1 have the same incubation times, and, therefore, these molecular types appear as a homogeneous group. MV2 and VV2 cases, when transmitted to mice with Val at position 129, induce the disease at the same post-inoculum intervals and thus suggesting similar biological properties of these sCJD strains. On the other hand, MM2 inocula show heterogeneous transmission properties and incubation times different from the above groups.

Based on the biochemical patterns obtained by combining the PrP27–30 core fragment and lower truncated PrP species, here we show three distinct groups of disease-associated PrP species in sCJD with type 1 PrP^{Sc}, MM2 subjects, and MV2/VV2 cases. Strikingly, similar molecular groups of PrP species are obtained by Satoh *et al.* (8) when combining truncated fragments of 11–12 kDa with type 1 and type 2 PrP27–30. Whether the present biochemical findings represent a molecular basis for different biological properties of the above sCJD strains remains to be determined.

Despite the recognition of conformational variants of disease-associated PrP species in experimental and naturally occurring prion diseases, little is known about the influence of different molecules on disease phenotype (24). Although it is commonly believed that PrP27–30 has a major role in modulating sCJD phenotype, it would be of interest to learn whether different truncated PrPs are related to specific clinical and pathological traits. Previous studies have disclosed that an internal PrP fragment of 7–8 kDa detected in patients with P102L Gerstmann-Sträussler-Scheinker disease (7, 25) and a C-terminal fragment associated with familial Creutzfeldt-Jakob disease due to E200K mutation (26) are toxic to neurons in combination with or in the absence of PrP expression (27, 28). Here we have found that a fully glycosylated PrP fragment, closely matching the C1 PrP^{C} fragment, was associated with amyloid plaques in MV2 cases and plaque-like PrP deposits in VV2 subjects. On the contrary, C1 PrP^{Sc} was not observed in sCJD subtypes lacking extracellular PrP deposition. It is noteworthy to emphasize that we also determined[2] the presence of C1 PrP^{Sc} in subjects with variant Creutzfeldt-Jakob disease (a condition characterized by florid PrP amyloid plaques) as well as in the newly identified bovine amyloidotic spongiform encephalopathy (BASE) (3) but not in amyloid-free typical bovine spongiform encephalopathy (BSE). Earlier studies have shown that C1 is a cell surface glycophosphoinositol-anchored protein starting at amino acid 110/111 in human neuroblastoma cells (6) and present under multiple truncation forms in brain tissue (17). According to our findings, it is conceivable that extracellular release of C1 PrP^{Sc} could be responsible for PrP deposition and aggregation, as observed in MV2 and VV2 sCJD subtypes. Altogether, these results show that PrP-truncated fragments may influence the disease phenotype of sCJD and that their characterization is important for the molecular definition of sCJD subtypes.

Acknowledgments—We thank Prof. Marina Bentivoglio for critical reading of the manuscript and Dr. Fabrizio Tagliavini for helpful suggestions.

REFERENCES

1. Prusiner, S. B. (1998) *Proc. Natl. Acad. Sci. U. S. A.* **95,** 13363–13383
2. Prusiner, S. B. (1997) *Science* **278,** 245–251
3. Casalone, C., Zanusso, G., Acutis, P., Ferrari, S., Capucci, L., Tagliavini, F., Monaco, S., and Caramelli, M. (2004) *Proc. Natl. Acad. Sci. U. S. A.* **101,** 3065–3070
4. Prusiner, S. B. (1992) *Biochemistry* **31,** 12277–12288
5. McKinley, M. P., Meyer, R. K., Kenaga, L., Rahbar, F., Cotter, R., Serban, A., and Prusiner, S. B. (1991) *J. Virol.* **65,** 1340–1351
6. Chen, S. G., Teplow, D. B., Parchi, P., Teller, J. K., Gambetti, P., and Autilio-Gambetti, L. (1995) *J. Biol. Chem.* **270,** 19173–19180
7. Jimenez-Huete, A., Lievens, P. M., Vidal, R., Piccardo, P., Ghetti, B., Tagliavini, F., Frangione, B., and Prelli, F. (1998) *Am. J. Pathol.* **153,** 1561–1572
8. Satoh, K., Muramoto, T., Tanaka, T., Kitamoto, N., Ironside, J. W., Nagashima, K., Yamada, M., Sato, T., Mohri, S., and Kitamoto, T. (2003) *J. Gen. Virol.* **84,** 2885–2893
9. Zou, W. Q., Capellari, S., Parchi, P., Sy, M. S., Gambetti, P., and Chen, S. G. (2003) *J. Biol. Chem.* **278,** 40429–40436
10. DeArmond, S. J., and Ironside, J. W. (1999) in *Neuropathology of Prion Diseases* (Prusiner, S. B., ed) pp. 585–652, Cold Spring Harbor Laboratory Press, Cold Spring Harbor, NY
11. Prusiner, S. B. (2001) *N. Engl. J. Med.* **344,** 1516–1526
12. Collins, S., Boyd, A., Fletcher, A., Kaldor, J., Hill, A., Farish, S., McLean, C., Ansari, Z., Smith, M., and Masters, C. L. (2002) *Ann. Neurol.* **52,** 115–118

[2] G. Zanusso, A. Farinazzo, and S. Monaco, unpublished observations.

13. Glatzel, M., Rogivue, C., Ghani, A., Streffer, J. R., Amsler, L., and Aguzzi, A. (2002) *Lancet* **360,** 139–141
14. Parchi, P., Castellani, R., Capellari, S., Ghetti, B., Young, K., Chen, S. G., Farlow, M., Dickson, D. W., Sima, A. A., Trojanowski, J. Q., Petersen, R. B., and Gambetti, P. (1996) *Ann. Neurol.* **39,** 767–778
15. Hill, A. F., Joiner, S., Wadsworth, J. D., Sidle, K. C., Bell, J. E., Budka, H., Ironside, J. W., and Collinge, J. (2003) *Brain* **126,** 1333–1346
16. Zanusso, G., Ferrari, S., Cardone, F., Zampieri, P., Gelati, M., Fiorini, M., Farinazzo, A., Gardiman, M., Cavallaro, T., Bentivoglio, M., Righetti, P. G., Pocchiari, M., Rizzuto, N., and Monaco, S. (2003) *N. Engl. J. Med.* **348,** 711–719
17. Zanusso, G., Righetti, P. G., Ferrari, S., Terrin, L., Farinazzo, A., Cardone, F., Pocchiari, M., Rizzuto, N., and Monaco, S. (2002) *Electrophoresis* **23,** 347–355
18. Zanusso, G., Farinazzo, A., Fiorini, M., Gelati, M., Castagna, A., Righetti, P. G., Rizzuto, N., and Monaco, S. (2001) *J. Biol. Chem.* **276,** 40377–40380
19. Wadsworth, J. D., Hill, A. F., Joiner, S., Jackson, G. S., Clarke, A. R., and Collinge, J. (1999) *Nat. Cell Biol.* **1,** 55–59
20. Parchi, P., Giese, A., Capellari, S., Brown, P., Schulz-Schaeffer, W., Windl, O., Zerr, I., Budka, H., Kopp, N., Piccardo, P., Poser, S., Rojiani, A., Streichemberger, N., Julien, J., Vital, C., Ghetti, B., Gambetti, P., and Kretzschmar, H. (1999) *Ann. Neurol.* **46,** 224–233
21. Parchi, P., Zou, W., Wang, W., Brown, P., Capellari, S., Ghetti, B., Kopp, N., Schulz-Schaeffer, W. J., Kretzschmar, H. A., Head, M. W., Ironside, J. W., Gambetti, P., and Chen, S. G. (2000) *Proc. Natl. Acad. Sci. U. S. A.* **97,** 10168–10172
22. Pan, T., Colucci, M., Wong, B. S., Li, R., Liu, T., Petersen, R. B., Chen, S., Gambetti, P., and Sy, M. S. (2001) *J. Biol. Chem.* **276,** 37284–37288
23. Korth, C., Kaneko, K., Groth, D., Heye, N., Telling, G., Mastrianni, J., Parchi, P., Gambetti, P., Will, R., Ironside, J., Heinrich, C., Tremblay, P., DeArmond, S. J., and Prusiner, S. B. (2003) *Proc. Natl. Acad. Sci. U. S. A.* **100,** 4784–4789
24. Lawson, V. A., Priola, S. A., Meade-White, K., Lawson, M., and Chesebro, B. (2004) *J. Biol. Chem.* **279,** 13689–13695
25. Tagliavini, F., Prelli, F., Ghiso, J., Bugiani, O., Serban, D., Prusiner, S. B., Farlow, M. R., Ghetti, B., and Frangione, B. (1991) *EMBO J.* **10,** 513–519
26. Capellari, S., Parchi, P., Russo, C. M., Sanford, J., Sy, M. S., Gambetti, P., and Petersen, R. B. (2000) *Am. J. Pathol.* **157,** 613–622
27. Forloni, G., Angeretti, N., Chiesa, R., Monzani, E., Salmona, M., Bugiani, O., and Tagliavini, F. (1993) *Nature* **362,** 543–546
28. Daniels, M., Cereghetti, G. M., and Brown, D. R. (2001) *Eur. J. Biochem.* **268,** 6155–6164

Identification of Distinct N-terminal Truncated Forms of Prion Protein in Different Creutzfeldt-Jakob Disease Subtypes

Gianluigi Zanusso, Alessia Farinazzo, Frances Prelli, Michele Fiorini, Matteo Gelati, Sergio Ferrari, Pier Giorgio Righetti, Nicolò Rizzuto, Blas Frangione and Salvatore Monaco

J. Biol. Chem. 2004, 279:38936-38942.
doi: 10.1074/jbc.M405468200 originally published online July 9, 2004
